



Gjøvik University College

HiGIA

Gjøvik University College Institutional Archive

Derawi, M. et al. (2011). Gait Recognition for Children over a Longer Period. In: Lecture Notes in Informatics, BIOSIG 2011, Proceedings - International Conference of the Biometrics Special Interest Group; 8.-9. September 2011 in Darmstadt, pp. 45-56. Bonn: Gesellschaft für Informatik.

*Please notice:
This is the copy of the book chapter*

*© Reprinted with permission from
Gesellschaft für Informatik*

Gait Recognition for Children over a Longer Period

Mohammad Omar Derawi¹, Hewa Balisane², Patrick Bours¹,
Waqar Ahmed³, Peter Twigg²

¹ Norwegian Information Security Laboratory,
Gjøvik University College, Norway
{mohammad.derawi,patrick.bours}@hig.no

² School of Engineering,
Manchester Metropolitan University, UK
hewa.balisane@hotmail.co.uk , p.twigg@mmu.ac.uk

³ Institute of Nanotechnology and Bioengineering,
University of Central Lancashire, UK
wahmed4@uclan.ac.uk

Abstract: In this paper a comparative investigation into the effects of time on gait recognition in children's walking has been carried out. Gait recognition has attracted considerable interest recently; however very little work has been reported in the literature which is related to gait recognition in children. It has been suggested ([Kyr02]) that the gait of children does not stabilize before they are 11 years old. In this paper we will provide arguments that support this suggestion. When looking at the performance of gait recognition, which serves as an indicator for the stability of gait, we found a relationship between performance improvement and aging of children. The gait of a group of children was measured twice with a 6 months period between the two measurements. Our analysis showed that the similarity between these two measurements is significantly lower than the similarity within each of the measurements. Finally we also report the effect of gender on performance of gait recognition.

1 Introduction

Even though gait analysis has a long history dating back to the time of Aristotle, who studied animal locomotion using artistic works, it was much later that work on the biomechanics of human walking was carried out at the end of the 19th century [Ari04, Pit09]. In recent years gait analysis has progressed rapidly with the development of more sophisticated electronics, advanced computer technology and more accurate sensors [GHS06]. A major interest in gait analysis involves its applications to bioengineering, physiotherapy, rehabilitation, the management of medical problems affecting the locomotor system and sports performance [YSS⁺07, SR09, JMOdG05, YMH⁺06]. More recently, it has also attracted considerable attention of researchers in identification and recognition for security and safety purposes [MLV⁺05, BS10]. Gait has a number of advantages over other forms of biometric features. For example, it is unique as each person has a distinctive walk, it is unobtrusive as gait avoids physical contact whilst collecting data unlike most other meth-

ods which involve physical touching; data can also be collected at a distance without the need for close proximity [CHH07, BCND01].

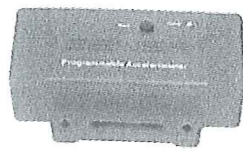
For improved security, gait analysis is being used for biometric authentication and identification [GSB06]. Currently, there are three types of systems being employed, which are machine vision based (MV), floor sensor based (FS) and wearable sensors (WS). Each type has its own unique advantages and disadvantages depending on the specific application being considered. The MV systems can be used remotely without any user interaction; however it is expensive and involves the use of background subtraction. FS based is very accurate but it is expensive to install and maintain. WS are simple, small and inexpensive devices and are not location dependent [GSB07]. These can be readily incorporated into mobile devices such as the popular i-Phone.

For adults of both genders, considerable research has been done on gait recognition and medical applications [DBH10, YTH⁺09, BS10, BN08]. However, with children very little work has been reported in the literature [PPW⁺97, OBC⁺99]. In previous studies we have reported an analysis of gait performance in children compared to adults [BDB⁺11b] and gait analysis under special circumstances [BDB⁺11a] such as variations in walking speed and carrying objects. In this paper we present a study on the effects of time on gait patterns in children and its relationships to gender and age. The accelerometer sensor was placed on the left side of hip. A comparative analysis of gait patterns in children and adults both male and female for the purposes of recognition and identification is presented.

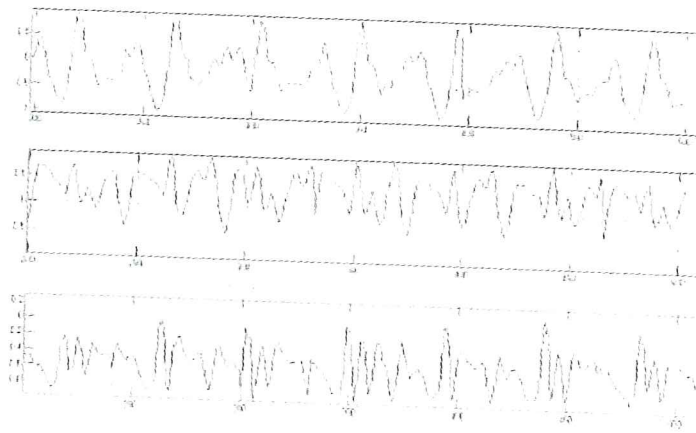
2 Experiment Design

In this study a programmable sensor (Model GP1, see Figure 1(a)) purchased from Sensr (USA, <http://www.sensr.com>) was programmed and used to record the motion of the children in several walking cycles. The GP1 measures the acceleration in three perpendicular directions which will be referred to as x , y and z . Figure 1(b) is an example of the output obtained from the GP1 sensor and shows the signals obtained in the x , y and z directions. These signals provided the raw data for the subsequent analysis reported in later sections of this paper. It is converted into a unique pattern for each individual for comparison. The GP1 can collect acceleration data up to $10g$ and has a sampling rate of 100 Hz per axis. Acceleration data is filtered inside the GP1 by a 2 pole Butterworth low pass filter with a cut-off frequency of 45 Hz [Sen07]. The device has a USB interface for transferring data and a 1 Mbyte memory for storage purposes. An overview of the specification of the Sensr GP 1 is given in Table 1.

In this study, 46 children (31 boys and 15 girls) with ages ranging between 5 to 16 years participated. Ethical approval was obtained from the school principal, the university's ethical approval committee and parents of the children. For each child, the parents formally approved participation in the study by signing a standard University approval consent form prior to volunteering. The criteria set for the child to take part of this study were that they should have no previous history of injury to the lower extremities within the past year, and no known musculoskeletal or neurological disease.



1. Initialize
2. Record
3. Download
4. Review



(a)

(b)

Figure 1: Left: SENSr GPI Device, Right: (x,y,z) Acceleration Output

Item	Specification
Size	3.935" x 2.560" x 1.140"
Weight with batteries	8.25 oz
Connectivity	USB
Accelerometer type	Programmable 3 axis MEMS
Accelerometer range	Programmable $\pm 2.5g$, $\pm 3.3g$, $\pm 6.7g$, $\pm 10g$
Sampling rate	100 Hz per axis
Memory type	Non-volatile EEPROM
Memory size	1 MByte
Device Temperature Range	$-20^{\circ}C$ to $+80^{\circ}C$

Table 1: Partial Specification of the GPI Sensor.

The Sensor was attached to left side of the hip (see Figure 2(a)) because previous studies have shown that the hip is the most stable position compared to leg, arm and other body positions. Volunteers were told to walk normally for a distance 17.5 meters in a carpeted hall on a flat surface in bare feet (see Figure 2(b)). At the end of the hall section the volunteers waited 5 seconds, turned round, waited 5 seconds and then walked back again.

This procedure was repeated twice and the data recorded was transferred to a PC for storage and analysis. The detailed sequence is as follows.

1. Connect to PC and initialise
2. Attach to the belt on the left hand side of the hip
3. Press the start recording button
4. Wait for 5 seconds

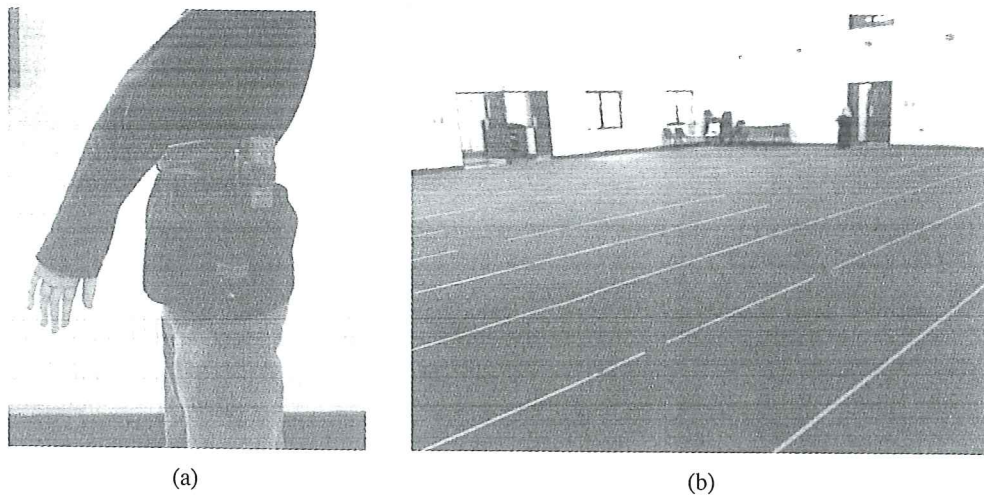


Figure 2: *Left: The Sensor Position, Right: Walking Hall*

5. Walk 17.5 meters from one end of hall section to the other
6. Stop and wait for 5 seconds
7. Turn around and wait for 5 seconds
8. Walk back 17.5 meters wait for 5 seconds and turn around
9. Repeat procedure

After walking twice the sensor was detached from the volunteer, connected to the computer and the data inside the GPI device was downloaded and stored and the file was named appropriately.

The main experiment was carried out over a time period of 6 months. First experiment was performed in September 2010 and the second was performed in March 2011. There were 20 volunteers who participated in the long term experiment out of an initial group of 46. In September 2010, each subject did 2 sessions, whilst 16 sessions were performed in March 2011. This means that each subject participated in 18 sessions in total.

3 Feature Extraction

The raw data retrieved from the Sensor sensor needs to be processed in order to create robust templates for each subject. The feature extraction steps are based on the work of [DBH10].

Preprocessing: First we apply *linear time interpolation* on the three axis data (x,y,z) retrieved from the sensor to obtain an observation every $\frac{1}{100}$ second since the time intervals between two observation points are not always equal. Another potential problem is that

the acceleration data from the sensor includes some noise. This noise is removed by using a *weighted moving average* filter (WMA). The formula for WMA with a sliding window of size 5 is given in Equation 1.

$$\frac{(a_{t-2}) + (2a_{t-1}) + (3a_t) + (2a_{t+1}) + (a_{t+2})}{9}, \quad (1)$$

where a_t is the acceleration-value in position t . The current value we are located at are given weight 3, the two closest neighbors weight 2 and the next two neighbors weight 1.

Finally we calculate the resultant vector or the so-called magnitude vector by applying the following formula,

$$r_t = \sqrt{x_t^2 + y_t^2 + z_t^2}, t = 1, \dots, N$$

where r_t , x_t , y_t and z_t are the magnitudes of resulting, vertical, horizontal and lateral acceleration at time t , respectively and N is the number of recorded observations in the signal.

Cycle Detection: From the data it is known that one cycle-length varies between 80 – 140 samples depending on the speed of the person. Therefore we need to get an estimation of how long one cycle is for each subject. This is done by extracting a small subset of the data and then comparing the subset with other subsets of similar lengths. Based on the distance scores between the subsets, the average cycle length is computed, as can be seen in Figure 3.

The cycle detection starts from a minimum point, P_{start} , around the center of the walk. From this point, cycles are detected in both directions. By adding the average length, denoted γ to P_{start} , the estimated ending point $E = P_{start} + \gamma$ is retrieved (in the opposite direction: $E = P_{start} - \gamma$). The cycle end is defined to be the minimum in the interval Neighbour Search from the estimated end point. This is illustrated in Figure 4. This process is repeated from the new end point, until all the cycles are detected. The end point in the Neighbour Search is found by starting from point E . From this point we begin searching 10% of the estimated cycle length, both before and after E for the lowest point. When the minimum point is found we store it into an array and we begin searching for the next minimum point by adding the length of one estimated cycle. When forward searching is complete we repeat this phase by searching backwards so all steps in the data are identified. We will therefore end up with having an array containing start/end index for each step. These points will therefore be used for the extraction of cycles, as illustrated in Figure 5.

Template Creation: Before we create the feature vector template, we ensure that cycles that are very different from the others are skipped. This is done by taking each cycle and calculating its distance compared to every other cycle by using dynamic time warping (DTW),

$$dtw_{i,j} = dtw(cycle_i, cycle_j)$$

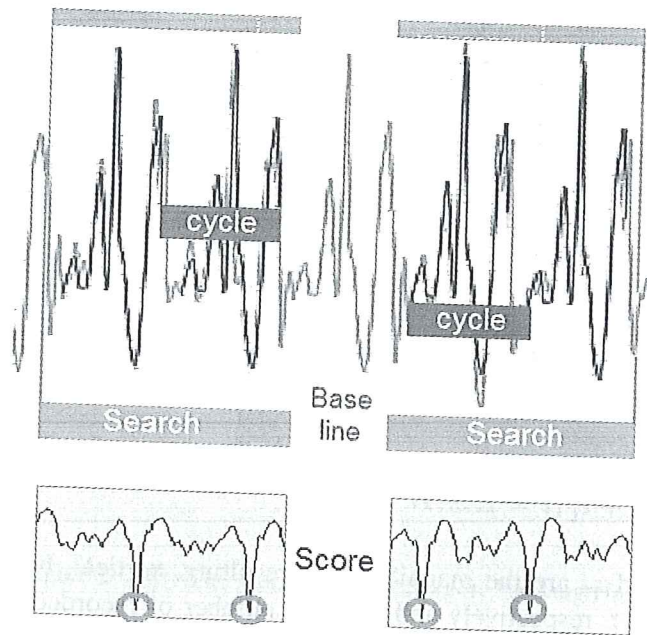


Figure 3: The yellow baseline area indicates the subset with 70 samples that are extracted, the green area is the search area where the baseline is compared against a subset of the search area. The 4 black subgraphs are the baseline at those points that has the lowest distance with the search area subsets, and the difference between them (blue area) indicate the cycle length [DBH10].

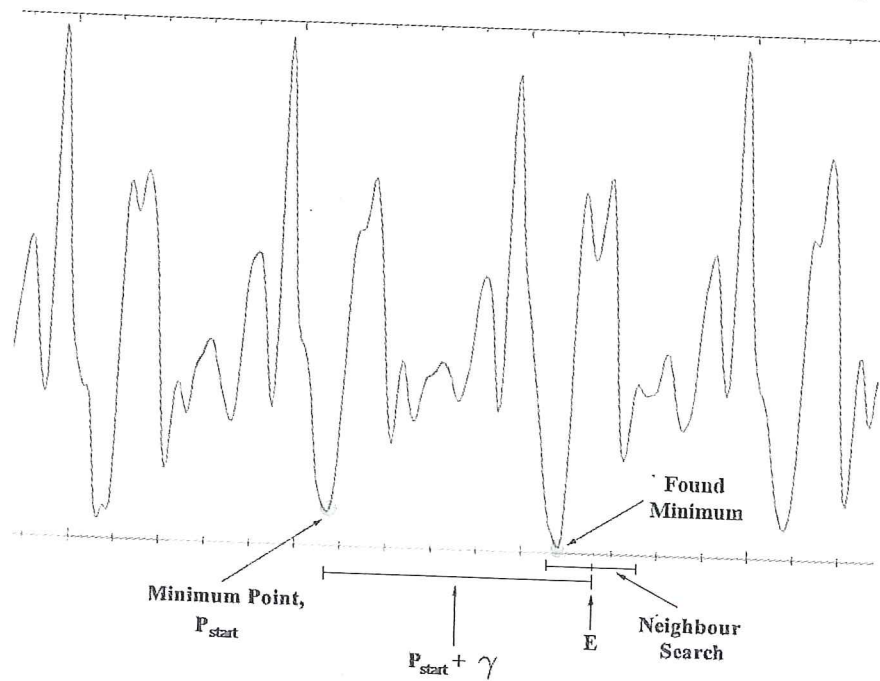


Figure 4: Cycle detection showing how each cycle (i.e the steps) in the resultant vector is automatically detected [DBH10].